# CORRELATION BETWEEN SOIL AMPLIFICATION AND RECORDED GROUND MOTIONS FOR TYPICAL LOCATIONS IN UTTARAKHAND

J.K. Mondal[1], N.H. Harinarayan[2], A. Kumar[3]

[1] *Research scholar, IIT Guwahati, joy.mondal@iitg.ac.in*
[2] *Research scholar, IIT Guwahati, n.harinarayan@iitg.ac.in*
[3] *Associate Professor, IIT Guwahati, abhiak@iitg.ac.in*

## *Abstract*

Amplification of incoming seismic waves by subsoil, termed as local site effects (LSE) plays a vital role in controlling the level of ground shaking during an earthquake (EQ). LSE depends on the soil type and the nature of bedrock motion. Ground response analysis (GRA) helps to quantify the LSE due to subsoil layers. To do so, bedrock motion or EQ records from a nearby outcrop recording station are essential. A major limitation in performing regional GRA in various seismically active regions of India is the lack of regional bedrock or nearby outcrop motion. In the present work, this limitation is addressed in two approaches, based on the analyses performed on 8 surface motion recording stations from Uttarakhand, India. Among these eight stations, four stations belong to NEHRP site class (SC) C, and the remaining stations belong to SC D. In the first approach, 30 globally recorded EQ motions, with varying ground motion parameters are considered as input for equivalent linear GRA (ELGRA). Results are obtained in the form of amplification factor (AF, defined as the ratio of peak amplitude of motion at the surface to the bedrock) versus Peak Horizontal Accelerlation (PHA). Being above selected motions from other parts of the globe and are not indicating regional seismic characteristics, in the second approach, firstly bedrock motions considering regional ground motion parameters are generated at above eight recording stations, using a stochastic method. Then based on generated bedrock motions and considering regional subsoil properties at each of the 8 recording station, GRA is done and AF versus PHA are determined for each of the earlier considered 8 recording stations. It must be mentioned here that few regional surface records are also available at above recording stations. In such case, AFs in the second approach are estimated based on simulated bedrock motion and recorded surface motions and thus without performing GRA. Thus, even though the first approach is based on global records, helps to understand the subsoil response for all possible future seismic scenarios. Similarly, the second approach being based on limited regional records as well as using simulated ground motions brings regional ground motion characteristics into the analyses. AF versus PHA from both the approaches match closely, for each of the 8 recording stations. A general observation from both the approaches suggests high PGA amplification for low PHA and low PGA amplification for high PHA. In addition, no significant amplification is observed beyond PHA of 0.3g and 0.2g for SC C and D respectively, clearly indicating that in case bedrock motion during probable future EQ generates PHA values mentioned above, the effect of local soil in amplifying bedrock motion will be no to minimal. Based on the above observations, two correlations between AF versus PHA for SC C and D each are proposed in this work. Proposed correlation can be used to understand the role of local soil for any level of input motion, for the region. Further, in seismic microzonation practice, where seismic hazard at bedrock as well as soil amplification are assigned weights and ranks separately. Presently developed correlation between the above two variables can also be helpful in deciding ranks of each of the two variables with respect to each other while estimating hazard index.

*Keywords: Ground response analysis; Site class; peak ground acceleration; amplification; bedrock motion*

## 1. Introduction

EQ related damages can be categorized as a function of surface seismic hazard that the EQ event produces. The bedrock level shaking can be estimated by performing seismic hazard analysis. The properties of bedrock motion can further be modified significantly by the local soil available at the site. Such modification in the bedrock motion due to the interaction seismic waves with the local soil is termed as local site effects (LSE). Thus, the effect of local soil must be taken into account to estimate surface level seismic hazard. This way, the surface seismic hazard is a collective function of three parameters namely; source, path and site effects. According to [1], LSE controls the ground level shaking scenario more than any other parameters. Further, researchers highlighted that LSE can be influential in modifying ground motions both for smaller and larger epicentral distance regions [2]. Building response during EQ is directly related to surface seismic hazard. Thus, in order to arrive at EQ resistant design parameters, quantification of LSE is necessary for locations near as well as far off from the the epicentre. LSE can be estimated numerically by performing GRA. Two important input parameters required to perform GRA are soil properties and bedrock motion. Soil properties include soil profile at the site, soil mass density ($\rho$), shear wave velocity ($V_s$), damping ratio ($\beta$), modulus degradation curve ($G/G_{max}$) and $\beta$ curve. For many important projects, site specific GRA are often conducted to estimate surface level seismic hazard [1,2]. In such site specific GRA, wave equation is solved by considering regional soil properties as well as bedrock motion characteristics for the site.

For majority of the locations in India, currently the site specific $G/G_{max}$ and $\beta$ curves are not available. Therefore, researchers [2–6] have adopted standard $G/G_{max}$ and $\beta$ curves [7–9] (developed for other regions) for performing site specific GRA. In addition, the recording of ground motions in India started only after mid-sixties and that too for very few river valley projects [10]. Therefore, in addition to non-availability of regional $G/G_{max}$ and $\beta$ curves, lack of regionally recorded bedrock motions is another challenge faced while performing region/ site specific GRA in India. Under such circumstances, in addition to consideration of standard $G/G_{max}$ and $\beta$ curves, globally recorded EQ motions such as 2001 Bhuj [4,11,12], 1999 Chamoli [5,6], 1989 Loma Prieta [11,13], 1989 Loma Gilroy, 1995 Kobe [11], 1971 San Fernando, 1987 Whittier Narrows [13], 1952 Kern County (Taft) [14] are praacticed while performing GRA. These motions many a times are scaled up/down [14] to match regional seismic hazard value. Further, the use of synthetic ground motions [15–18] or recorded ground motions modified to match with uniform hazard spectra [12], are also practiced. It should be highlighted here that the adopting ground motion records from other other regions may not represent true seismicity of the region under consideration. Further, adopting limited number of EQ records may not represent all possible seismic scenarios likely to be experiences by the site in the future. To overcome such limitations, a larger number of seismic scenarios, capable of covering wider range of ground motion parameters, must be taken into account while performing GRA [2].

In the lack of regional ground motion records at bedrock, present study attempts to understand the overall response of soil available at 8 recording stations located in Uttarakhand, India based on two approaches, discussed later, to give an overall picture of LSE for the region. Recording stations considered in this study are; Tanakpur (TA), Kotdwar(KO), Haldwani (HA), Vikashnagar (VI), Khatima (KH), Kashipur (KA), Roorkee (RO), Udhamsinghnagar (UD).

## 2. Study area

Present study considers eight surface recording stations located adjacent to Himalayan belt in Uttarakhand, India. The entire study area considered here is bounded by Main Central Thrust (MCT) and Main Boundary Thrust (MBT). The study area encompasses the region located between 77ºE-82ºE longitude and 28ºN-32ºN latitude. It should be highlighted here, the study area has encountered two strong EQs in recent past namely, 1991 Uttarkashi EQ ($M_w$ 6.8) and 1999 Chamoli EQ ($M_w$ 6.6). Both of these EQs were responsible for extensive damages in the form of loss of Human lives and infrastructure [19]. In addition, during the 1803 Kumaon- Nepal EQ and 1905 Kangra EQ also, the study area was subjected to intense seismic hazard [19]. The state of Uttarakhand is home to a population about 0.1 billion (as per census 2011). Further, the traditional houses in this part of India, is made of mud, brick and stones which can be vulnerable to future EQ damages. Keeping in mind the high population density in north India and considerable depth of overburden in the region, not only the bedrock motion but surface motion during the future EQ will cause high to very high seismic hazard as well as manifold increase in the extent of damage in comparison to past experiences.

### 2.1 Existing EQ records

EQ records obtained in a region from past EQs are essential to predict the ground motion characteristics of a future EQ in the region. These EQ records are useful for the assessment of seismic hazard and for the quantification of induced effects as well. Though the strong motion program in India started in mid-sixties of twenty century, it received a significant boost only in 2004 when Department of Science and Technology (DST) Government of India, sanctioned a project titled "National Strong Motion Instrumentation Network" (NSMIN) to Department of Earthquake Engineering (DEE), Indian Institute of Technology, Roorkee (IITR). Under this project, about 300 state of art digital accelerographs were installed in North and North-Eastern India located in seismic zone IV, V and even in some of the highly populated cities located in zone III [10,20,21]. EQ recordings and information regarding the recording stations are monitored by "Program for Excellence in Strong Motion Studies" (PESMOS). All the recording stations under PESMOS are controlled by DEE, IITR.

Table 1-Details of recording stations (as per [21])

| **KH** | GWT at 3m | **KO** | GWT at 160m | **KA** | GWT at 3m | **HA** | GWT at 160m |
|---|---|---|---|---|---|---|---|
| Depth (m) | Soil description | Depth (m) | Soil description | Depth (m) | Soil description | Depth (m) | Soil description |
| 1.5 | Clay, sand | 1.5 | Clay, sand, boulders | 3 | Clay | 1.5 | Clay, sand, boulders |
| 10 | Clay, sand, boulders | | | 10 | Pebbles, clay, soft boulders | | |
| 30 | Loose boulders, fine sand | 30 | Boulders, pebbles, sand | 30 | Fine sand, clay | 30 | Boulders, pebbles, sand |
| **RO** | GWT at 6m | **TA** | GWT at 12m | **UD** | GWT at 3m | **VI** | GWT at 25m |
| Depth (m) | Soil description | Depth (m) | Soil description | Depth (m) | Soil description | Depth (m) | Soil description |
| | | 3 | Clay, sand , boulders | 3 | Clay | 1.5 | Clay |
| 10 | Silty sand | 10 | Boulders, pebbles, sand | 10 | Pebbles, clay, soft boulders | 10 | Clay, boulders |
| 30 | Sand | 30 | Boulders, fine sand | 30 | Sand, clay | 30 | Pebbles, boulder, sand |



 

These database are available on the website "www.pesmos.in". It must be mentioned here that though regional ground motion records are available at each of the above 8 recording stations, these records cannot be used as bedrock motion for the present study as the recording stations are located on SC C and D (with considerable site effect component) as mentioned earlier.

### 2.2 Subsoil lithology

Above mentioned eight recording stations (TA, KO, HA, VI, KH, KA, RO, UD), considered in the present study, are located in Tarai (Foot plains of the Himalaya) region of Uttarkhand state, India. In general, the subsoil of the Tarai region consists of alluvial fill deposits. Further, a detailed description of the subsoil condition, for each of the stations is given in Table 1 (as per [21]). It can be observed from Table 1 that the subsoil lithologies for all the 8 rcording stations are dominated by the presence of sand, clay, pebbles and boulders. Further, the top 30m subsoil lithology for all the stations, except KO and HA, can be divided into two distinct layers which span from the surface to 10m depth and 10m to 30m depths respectively (Table 1). The top layer at RO station consists of silty sand, whereas top layers at other stations are further sub-divided into a combination of different sub-layers of clay, sand, pebbles and soft boulders (Table 1). On the other hand, the bottom layers (10m-30m) at all the recording stations, except for KO and HA, consist of individual layer made of either sand, clay, pebbles, or a combination of these. Further, the locations of ground water table (GWT) at 6 recording stations (TA, VI, KH, KA, RO, UD) are between 3m and 25m (Table 1). At the KO and HA stations, the lithologies are similar and consisting of clay, sand, and boulders in the top 1.5m depth. Below this depth, one layer consisting of sand, pebbles and boulder extends to 30m depth. At both of these recording stations (KO and HA), GWT is located at a depth of 160m [21].

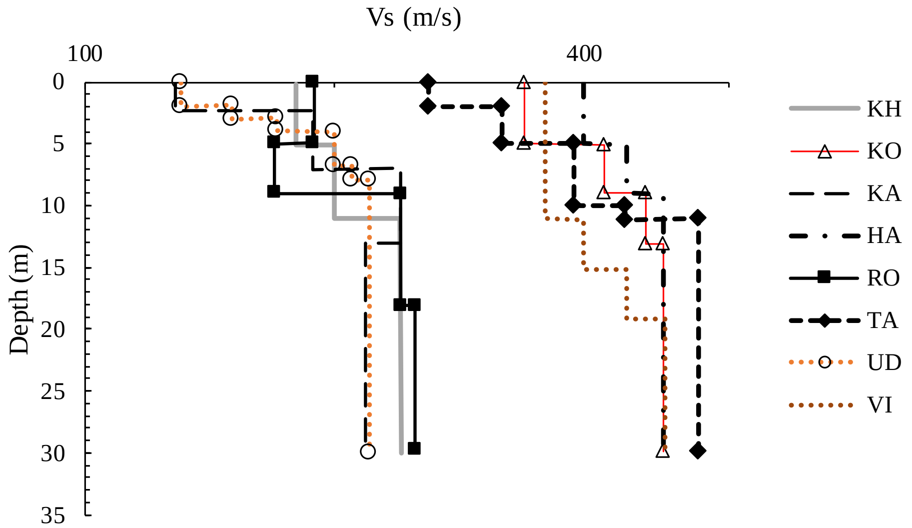


Fig. 1 - Vs Profile of the recording stations (as per [21])

### 2.3 Site characterization

SC information for each recording station is given on PESMOS website (www.pesmos.in). It must be mentioned here that PESMOS given SC [22] are based on the physical description of soil and average $V_s$ value in the top 30m soil ($V_{s30}$). According to PESMOS, sites with $V_{s30}$ > 700m/s, are classified as SC A or firm/ hard rock site; sites with 375m/s < $V_{s30}$ < 700m/s are classified as SC B or soft to firm rock site; and sites with $V_{s30}$ < 375m/s are classified as SC C or soil sites. As per [10], SCs assigned to the recording stations by PESMOS are only the physical description of the soil. According to SC given by PESMOS, while KO station belong to SC B, rest all 7 stations considered in this work, belong to SC C. Later, [21] conducted Multi-channel analysis of surface wave (MASW) at all the 8 sites (each adjacent to each recording station considered in this work) and concluded that TA, KO, HA and VI belong to SC C, stations (KH, KA, RO and UD) belong to SC



 

D, following NEHRP site classification scheme [23]. The $V_s$ profiles for all the 8 sites as per [21] are shown in Fig.1.

## 3. Equivalent linear GRA (ELGRA)

LSE can be correlated collectively to bedrock motion and near-surface geology by performing GRA. Further, while performing GRA, the choice of GRA methodology depends on the expected level of shear strain ($\gamma$) in the soil. equivalent linear GRA (ELGRA) is valid for a maximum $\gamma$ range of 0.1-0.3%. On the other hand, when $\gamma$ exceeds 0.2-0.5%, non-linear GRA with excess pore water pressure generation/dissipation model is preferred. However, due to simplicity and computational efficiency, ELGRA is most frequently preferred among the researchers. In this study as well, ELGRA is performed for the assessment of LSE. As mentioned earlier, bedrock motion and dynamic soil properties curve (or DSPC consisting of $G/G_{max}$ and $\beta$ curves) of each soil layer, are essential input parameters for ELGRA. Hence, in the subsequent sections, details of bedrock motion and DSPCs, considered for the present study, are discussed.

### 3.1 Choice of bedrock motion

Ground motion properties such as amplitude, frequency content, duration are responsible for the modification of input ground motion. Thus, while attempting to asses LSE for a particular site, bedrock motions should be chosen in a manner that all the uncertainties related to ground motion properties must be taken into account. Keeping in mind the importance of bedrock motion and nonavailability of regional ground motion records as mentioned earlier, thirty globally recorded ground motions that were selected by [2], are considered in this work. Details of selected ground motions are presented in Table 2. It can be observed from Table 2, the thirty ground motions considered for the present work have a wide variation in amplitude content as the PHA varies between 0.008g and 1.03g. Further, predominant frequency of ground motions varies from 0.26Hz to 16.5Hz (see Table 2). Additionally, selected ground motions consist of both short length records (such as 7sec) and long length records (such as 140sec) as can be observed in Table 1. Referring to the tectonic setting to Uttrakhand region discusse earlier, region is potential of seismic hazard both from regional as well as distant faults. Selected ground motions in this work belong to epicentral distance varying from 1km to 216km [2] and magnitude from 5.0 -8.1 ($M_w$) as reported by [2], thus representing both near and far distance seismic scenarios.

Table 2-Details of selected Ground motions (as per [2])

| Sr. No. | Ground Motion Details | PGA (g) | Duration (s) | Predominant Frequency (Hz) |
|---|---|---|---|---|
| 1 | ADAK, ALASKA 1971-M 6.8;R-67KM, N81E | 0.098 | 24.58 | 3.32 |
| 2 | ANCHORAGE, ALASKA 1875, M-6, R81-GOULE HALL STATION | 0.036 | 18.59 | 5.42 |
| 3 | ANCHORAGE ALASKA 1975, M 6, R 79, WESTWARD HOTEL STATION (BASEMENT) | 0.049 | 38.96 | 1.00 |
| 4 | ANZA 02/25/80, BORREGO AIR BRANCH 225 | 0.046 | 10.25 | 2.39 |
| 5 | ANZA 02/25/80 1047, TERWILLIGER VALLEY 135 | 0.080 | 10.01 | 6.54 |
| 6 | BISHOP-ROUND VALLEY 11/23/84 1914, MCGEE CREEK SURFACE 270 | 0.075 | 6.80 | 3.9 |
| 7 | BORREGO MOUNTAIN 04/09/68 0230, EL CENTRO ARRAY 9, 270 | 0.056 | 39.95 | 0.46 |
| 8 | BORREGO MOUNTAIN 04/09/68 0230, PASADENA-ATHENAEUM, 270 | 0.009 | 60.23 | 0.61 |



 

| Sr. No. | Ground Motion Details | PGA (g) | Duration (s) | Predominant Frequency (Hz) |
|---|---|---|---|---|
| 9 | BORREGO MOUNTAIN 04/09/68 0230, TERMINAL ISLAND, 339 | 0.008 | 51.80 | 2.50 |
| 10 | CAPE MENDOCINO EARTHQUAKE RECORD 04/25/92, MW-7.0, 90 DEG COMPONENT | 1.03 | 59.98 | 4.44 |
| 11 | CHALFANT 07/20/86 1429, BISHOP PARADISE LODGE,070 | 0.046 | 39.95 | 16.5 |
| 12 | CHILE EARTHQUAKE, VALPARAISO RECORD, 3/3/85 | 0.120 | 79.39 | 2.1 |
| 13 | COALINGA 05/02/83 2342 PARKFIELD, FAULT ZONE 6/ 090 | 0.055 | 39.95 | 0.43 |
| 14 | COALINGA 05/09/83 PALMER AVE ANTICLINE RIDGE, 090 | 0.215 | 40.00 | 2.29 |
| 15 | GEORGIA, USSR 06/15/91 0059, BAZ X | 0.033 | 34.07 | 1.22 |
| 16 | IMPERIAL VALLEY 10/15/79 2319, BONDS CORNER 230 | 0.100 | 19.88 | 1.41 |
| 17 | KERN COUNTY 7/21/52 11:53, SANTA BARBARA COURTHOUSE 042 | 0.086 | 75.35 | 1.84 |
| 18 | KOBE 01/16/95 2046, ABENO 000 | 0.22 | 139.98 | 0.26 |
| 19 | KOBE 01/16/95 2046, KAKOGAWA 000 | 0.250 | 40.91 | 0.91 |
| 20 | KOBE 01/16/95, KOBE PORT ISLAND 090 | 0.530 | 42 | 0.79 |
| 21 | LIVERMORE 01/27/80 0233, HAYWARD CSUH STADIUM 236 | 0.027 | 15.98 | 3.61 |
| 22 | LIVERMORE 01/27/80 0233 LIVERMORE MORGAN TERR PARK 265 | 0.197 | 24 | 5.61 |
| 23 | LOMA PRIETA TA 10/18/89 00:05, ANDERSON DAN DOWNSTREAM 270 | 0.240 | 39.59 | 2.14 |
| 24 | LOMA PRIETA TA 10/18/89 00:05, HOLLISTER DIFF ARRAY 255 | 0.270 | 40 | 1.48 |
| 25 | MICHIOACAN EARTHQUAKE 19/9/85, CALETA DE CAMPOS, N-COMPONENT | 0.140 | 81.06 | 1.39 |
| 26 | NORTHERN CALIFORNIA 09/22/52 1141, FERNDALE 134 | 0.070 | 40 | 1.31 |
| 27 | NORTHRIDGE EQ 1/17/94 1231, ANACAPA ISLAND | 0.013 | 40 | 4.46 |
| 28 | NORTHRIDGE EQ 1/17/94 1231, ARLETA 360 | 0.310 | 39.94 | 1.46 |
| 29 | PARKFIELD 06/28/66 04:26, CHROME # 8 | 0.116 | 26.09 | 0.85 |
| 30 | TRINIDAD 11/08/08, 10:27, RIO DEL OVERPASS E | 0.130 | 22.0 | 3.14 |



 

### 3.2 Choice of DSPCs

Soil is a highly complex material that exhibits non-linearity in shear stress ($\tau$)- $\gamma$ behavior at very moderate to high $\gamma$ level. During an EQ, the $G$ and $\beta$ values of the soil vary continuously with the development of different $\gamma$ levels. While performing ELGRA, the $G$ and $\beta$ values can be updated by utilizing DSPC. Theoretically, these site-specific DSPCs should be obtained for each soil type and condition in the laboratory through extensive experimentation. However, due to the non-availability of such site specific DSPCs for the selected stations, standard DSPCs are being considered for the present study. These standard DSPCs for a soil can be selected based on soil type, OCR and PI. For the present study, the silty sand and sand layers shown in Table 1, are modeled based on $G/G_{max}$ and $\beta$ curves proposed by [7] for average sand. Similarly, clay soils shown in Table 1, are modeled as per $G/G_{max}$ and $\beta$ curves proposed by [7] for clay (upper bound). The boulder/pebble layers are modeled with $G/G_{max}$ and $\beta$ curves developed for gravel by [24].

### 3.3 Analysis

ELGRA is carried out for each of the 8 soil profiles shown in Table 1 and for of the thirty ground motions (see Table 2). In total, 30x8 = 240 ELGRAs are performed using the MATLAB code developed by [25]. For the modeling purpose, each of the eight soil profiles (see Table 1) are subdivided into different layers of thicknesses not more than 2.5m. Initial $V_s$ values for all the layers are taken as per Fig. 1. Initial $\beta$ values for all the layers are considered as 1%. $\rho$ values are assumed referring to standard values for clay, sand, pebbles and boulders, keeping in mind initial $V_s$ values. Further, three types of DSPCs as mentioned in the last subsection, are used. All the ground motions are applied at the bottom of the soil profiles (see Table 1) and results are obtained in the form of acceleration time histories at the surface. Subsequently, AF values between the base and the top of the profile are obtained and the corresponding PHA values are also noted for each profile subjected to each input motion.

## 4. Synthetic ground motions

Ground motion simulation using stochastic finite fault model (eg. [26,27]) provides a powerful tool for seismic hazard analysis in regions having sparce ground motion records. Plethora of studies around the globe have highlighted the efficacy of finite fault model in simulating ground motion records (eg. [28–30]). In section 3.1 earlier, 30 ground motions from global database are used in the absence of regional ground motion records at bedrock. In this section, keeping in mind that earlier considered 30 ground motions are from different parts of globe and not regional records, additional set of ground motions generated synthetically using regional ground motion model parameters of the present study area, are also used for GRA. This way, the response of regional soil, corresponding to ground motions from region as well as other parts of globe, both are used. To do so, FORTRAN code EXSIM (Extended Finite-Fault Simulation) based on the EXSIM model, developed by [26] is used to generate synthetic ground motion. EXSIM model is based on the concept of dynamic corner frequency ($f_0$) that comprehends $f_0$ as a time-dependent parameter. Detail information on EXSIM model can be found in [26], and is not discussed here.

It must be mentioned here that the EQ used for bedrock motion simulation is the same for which surface motion at the recording station is known. Details of input paramters used for the simulation of EQ ground motion are presented in Columns 2 and 3 of Table 3. Table 4 summarized PHA based on simulated ground motion and corresponding PGA based on recorded ground motion for each of the recording station. This way another set of AF(as the ratio of PGA and PHA) versus PHA are obtained. It can be observed from Table 4 the PHA values of the simulated ground motions are very less. In order to compare AF versus PHA based on regional records with the one obtained based on global records, additional two scenario bedrock motions corresponding to magnitude 7 and 7.5 $M_w$, are simulated here (details can be found in Columns 4 and 5 of Table 3). The PHA values for scenario motions are 0.306g and 0.92g for magnitude 7 and 7.5 $M_w$ respectively. For both scenario EQs, firstly soil profiles discussed in section 3 are used to determine AF at each recording station and then AF versus PHA variation (colelctively based on regional ground motion records as well as scenario EQs) is compared with the one obtained in section 3.



 

Table 3-Details of input parameters

| Parameters (1) | 4/4/2011 Event (2) | 5/03/2012 (3) | Scenario EQ 1 (4) | Scenario EQ 2 (5) |
|---|---|---|---|---|
| Magnitude ($M_w$) | 5.7 | 4.9 | 7 | 7.5 |
| Stress drop | 21MPa [31] | 10.7MPa [31] | 30MPa | 35MPa |
| Crustal density ($\rho$) | 2.71g/cc [32] | | | |
| Crustal shear-wave velocity ($\beta_s$) | 3.5km/s [33] | | | |
| Kappa | 0.05 [28] | | | |
| Quality factor | $Q_s = (155)f^{(0.927)}$[34] | | | |
| Geometric spreading | $Gs[f,R] = \begin{bmatrix} 1/\sqrt{R} & \mathrm{R} \quad R < 100 \leq 100\ \mathrm{km} \\ 1/\sqrt{100R} & \mathrm{R} > 1\mathrm{R} > 00\ \mathrm{km} \end{bmatrix}$ [35] | | | |
| Rupture propagation speed | 0.8 $\beta_s$ [36] | | | |

Table 4-Details of recorded ground motion

| Stations | TA | KO | HA | VI | KH | KS | RO | UD |
|---|---|---|---|---|---|---|---|---|
| EQ | 4/4/2011 | 4/4/2011 | 5/03/2012 | 5/03/2012 | 4/4/2011 | 4/4/2011 | 4/4/2011 | 4/4/2011 |
| PGA (g) | 0.012232 | 0.006626 | 0.005912 | 0.002039 | 0.020387 | 0.009174 | 0.003568 | 0.009174 |
| PHA (g) | 0.007747 | 0.001529 | 0.000306 | 0.000102 | 0.005097 | 0.001672 | 0.001172 | 0.000673 |

## 5. Results and discussion

Based on the analyses done earlier in this paper, AFs are obtained based on ELGRA and through comparison of simulated bedrock motion with recorded surface motion, and scenario EQs and ELGRA. AFs or range of AFs for different cities in India were reported by various researchers [11,13–15]. Authors want to highlight that the AF which in other words represents LSE from a site, is also a function of PHA. Therefore, assigning a particular value of AF or a range of AFs to a site may not be justified as future seismic scenario if changes, will alter the AF values as well. Thus, rather than proposing value or range of AF for a site/ region, if some correlations between AF and PHA can be developed, that will give a more broader picture of LSE. Keeping this in mind, AFs based on all 240 ELGRAs done in section 3 along with corresponding PHA values are used for developing correlation. Two correlations are developed separately for SC C and D each based on the analyses results.

AFs obtained for stations corresponding to SC C (TA, KO, HA and VI) are plotted against their respective PHA values as shown in Fig. 2. In general, low value of AF is obtained for high PHA value and vice-versa. The maximum and minimum value of AFs obtained in this study for SC C is 7.17 and 0.68 respectively. Based on the variation pattern (see Fig. 2), following correlation between AF and PHA is proposed in this study;

$$AF = 1.132(PHA)^{-0.302} \quad (1)$$



 

Similarly, AF values obtained for recording stations belonging to SC D (KH, KA, RO and UD) are also plotted against their respective PHA values in Fig. 3. For SC D, the maximum and minimum values of AFs are obtained as 3.56 and 0.27 respectively. Based on the variation pattern, following correlation between AF and PHA is proposed in this work;

$$AF = 0.4823(PHA)^{-0.42} \quad (2)$$

It can be observed collectively from Figs. 2 and 3 that for PHA range of 0.2-0.3g, the AF values become equal to unity irrespective of SC. Further, in case of PHA>0.5g, AFs are obtained even lesser than 1. In addition, AFs corresponding to SC C are higher than AFs corresponding to SC D (see Figs. 2 and 3). It should be highlighted here, high value of PHA is responsible for development of high $\gamma$ in soil. At high $\gamma$, soil behaves non-linearly. Such non-linear behaviour of soil at high $\gamma$ is governed by $\beta$ alone [2]. From the observation of different standard $\beta$ curves ([7,9,24]), it is well known that at high $\gamma$, the corresponding $\beta$ value is also very high. Therefore, for ground motions with high PHA (or at high $\gamma$), influence of high value of $\beta$ becomes predominant in controlling soil response. Consequently, de-amplification is observed for ground motions with PHA>0.5g. This justification is valid for different SCs too. Since SC C consist of stiffer soil compared to SC D, it is subjected to low $\gamma$ value and, subsequently higher AFs. For SC D however, soil experiences high value $\gamma$ due to presence of soft material, which leads to less value of AFs.

It should be highlighted here, the correlations developed between PHA and AF in the present study are based on thirty globally recorded ground motions and ELGRA. In order to validate the outcome of the present study, the AFs determined based on recorded surface motions and simulated bedrock motions for the respective stations are also presented in Fig 2 and 3. It can be observed from Figs. 2 and 3 that the AFs obtained from recorded surface motions and simulated bedrock motions are following the trend used in developing the proposed correlations for SC C and D. It must be mentioned here that initial simulations for which surface record is available had very low PHA (see Table 4) and thus two scenario EQs which are simulated additionally covers higher PHA range. AF versus PHA obtained based on global EQs as well as simulated EQs and regional surface records matches very well for both SCs. Hence, it can be said that in the absence of regional recorded ground motions for bedrock condition, selected 30 global records could capture LSE very effectively.

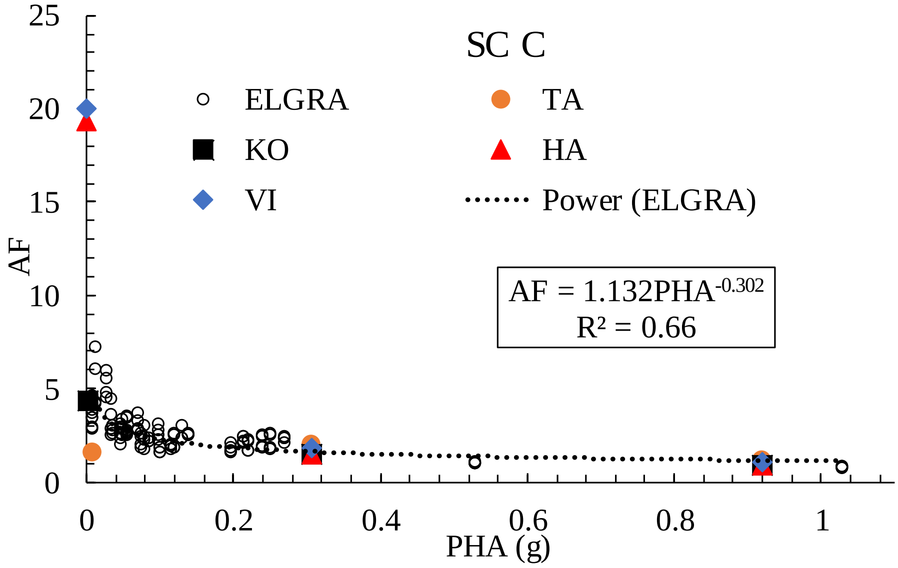


Figure 2-Correlation between AF and PHA for SC C



 

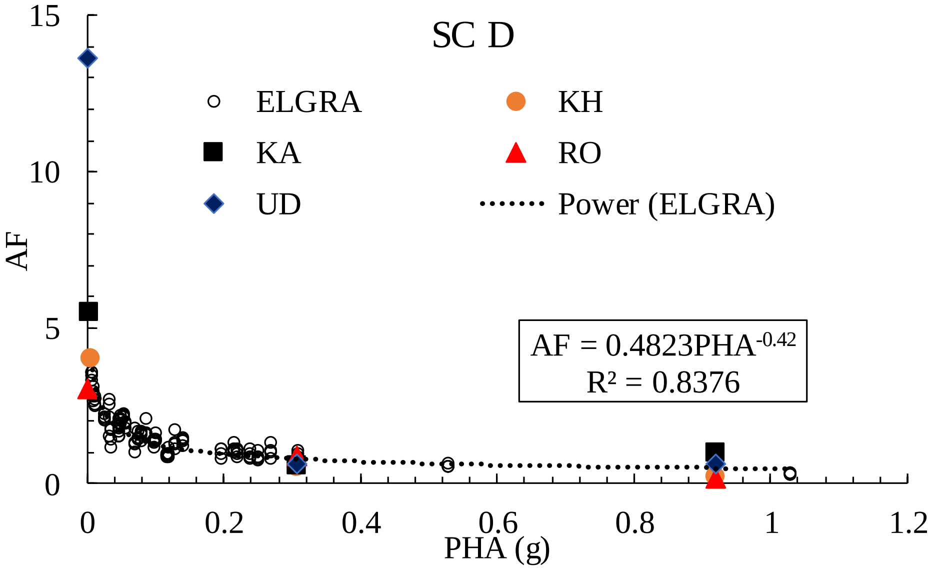


Figure 3-Correlation between AF PHA for SC D

## 6. Conclusion

LSE plays an important role in controlling the EQ damage scenario at a particular site. Thus, quantification of LSE is necessary while assessing surface seismic hazard values. Present study focuses on estimating LSE through the determination of AFs. In the absence of regional bedrock motions, 30 globally recorded ground motions are bedrock conditions are considered and based on ELGRA, LSE in terms of AF versus PHA for 8 recording stations from Uttarakhand region, India is assessed. Based on the variation pattern, two empirical correlations between AF and PHA are proposed for SC C and D. Being ground motions selected above are from other parts and not regional, regional ground motion records are also simulated for bedrock condition using regional ground motion model parameter. In this case, AF based on surface known record and bedrock simulated ground motions are estimated. Since these simulated ground motions could only validate AF versus PHA variation for very low PHA, additionally two EQ scenarios are alsod developed for higher PHA. Based on site-specific soil profile and using scenario EQ generated bedrock motions, AF at each of the 8 recording stations are estimated as a function of PHA. Comparison of AF based on known surface record as well as ELGRA for scenario EQs with AF versus PHA based on global records show well matching. Further, it is observed that for PHA>0.5g, the LSE in amplifying bedrock motion will not be there. Both proposed correlations can be very helpful in determining hazard index taking bedrock motion and corresponding AF into account which performing seismic microzonation studies.

## 7. References

[1] Anbazhagan P, Prabhakaran A, Madhura H, Moustafa SSR, Al-Arifi NSN (2017): Selection of representative shear modulus reduction and damping curves for rock, gravel and sand sites from the KiK-Net downhole array. Natural Hazards, 88 (3), 1741–1768. https://doi.org/10.1007/s11069-017-2944-x.

[2] Kumar A, Baro O, Harinarayan NH (2016): Obtaining the surface PGA from site response analyses based on globally recorded ground motions and matching with the codal values. Natural Hazards, 81 (1), 543–572. https://doi.org/10.1007/s11069-015-2095-x.

[3] Ranjan R. Seismic Response Analysis of Dehradun (2005): International Institute for Geo-Information Science and Earth Observations -Enschede, Netherlands, P-86.

[4] GovindaRaju L, Ramana G V., HanumanthaRao C, Sitharam TG (2004): Site-specific ground response analysis. Current Science, 87 (10), 1354–1362.

[5] Mahajan AK, Sporry RJ, Ray PKC, Ranjan R, Slob S, Van Cees W (2007): Methodology for site-response studies



 

using multi-channel analysis of surface wave technique in Dehradun city. Current Science, 92 (7), 945–955.

[6] Mohanty WK, Walling MY, Nath SK, Pal I (2007): First order seismic microzonation of Delhi, India using geographic information system (GIS). Natural Hazards, 40 (2), 245–260. https://doi.org/10.1007/s11069-006-0011-0.

[7] Seed H, Idriss I (1970): Soil moduli and damping factors for dynamic response analysis. University of California, Berkeley.

[8] Sun J, Golesorkhi R, Seed H (1988): Dynamic moduli and damping ratios for cohesive soils. Report No EERC 88-15. University of California Berkeley.

[9] Gazetas G, Fan K, Tazoh T, Shimizu K (1973): Seismic Response of the Pile Foundation of Ohba-Ohashi Bridge. 3rd International Conference on case Histories in Geotechnical Engineering, St. Louis, p. 1803–1809.

[10] Mittal H, Kumar A, Ramhmachhuani R (2012): Indian National Strong Motion Instrumentation Network and Site Characterization of Its Stations. International Journal of Geoscience, 3 (6), 1151–1167. https://doi.org/10.4236/ijg.2012.326117.

[11] Phanikanth VS, Choudhury D, Reddy GR (2011): Equivalent-Linear Seismic Ground Response Analysis of Some Typical Sites in Mumbai. Geotechnical and Geological Engineering, 29 (6), 1109–1126. https://doi.org/10.1007/s10706-011-9443-8.

[12] Shukla J, Choudhury D (2012): Seismic hazard and site-specific ground motion for typical ports of Gujarat. Natural Hazards, 60 (2), 541–565. https://doi.org/10.1007/s11069-011-0042-z.

[13] Govindaraju L, Bhattacharya S (2012): Site-specific earthquake response study for hazard assessment in Kolkata city, India. Natural Hazards, 61 (3), 943–965. https://doi.org/10.1007/s11069-011-9940-3.

[14] Boominathan A, Dodagoudar GR, Suganthi A, Uma Maheswari R (2008): Seismic hazard assessment of Chennai city considering local site effects. Journal of Earth System Science, 117(suppl 2), 853–863. https://doi.org/10.1007/s12040-008-0072-4.

[15] Anbazhagan P, Sitharam TG (2008): Seismic microzonation of Bangalore, India. Journal of Earth System Science, 117(suppl 2), 833–852. https://doi.org/10.1007/s12040-008-0071-5.

[16] Kamatchi P, Ramana GV, Nagpal AK (2008): Site-Specific Analysis Of Delhi Region For Scenario Earthquakes. 14th World Conference on Earthquake Engineering, Beijing, China.

[17] Kanth STGR (2009): Esimation of Site Amplification Factors for Guwahati City. Indian Geotechnical Conferenece, Guntur, India. pp. 527–530.

[18] Rao Chappidi H, Ramana GV (2009): Site specific ground response analyses at Delhi, India. Electronic Journal of Geotechnical Engineering, 14(D)

[19] Harinarayan NH, Kumar A (2018): Seismic Site Classification of Recording Stations in Tarai Region of Uttarakhand , from Multiple Approaches. Geotech Geol Eng;36:1431–46. https://doi.org/10.1007/s10706-017-0399-1.

[20] Kumar A, Mittal H, Sachdeva R, Kumar A (2012): Indian strong motion instrumentation network. Seismological Research Letter, 83 (1), 59–66. https://doi.org/10.1785/gssrl.83.1.59.

[21] Pandey B, Jakka RS, Kumar A (2016): Influence of local site conditions on strong ground motion characteristics at Tarai region of Uttarakhand, India. Natural Hazards, 81 (2), 1073–1089. https://doi.org/10.1007/s11069-015-2120-0.

[22] Borcherdt RD (1976): Estimates of Site-Dependent Response Spectra for Design (Methodology and Justification). Earthquake Spectra, 10 (4), 617–653. https://doi.org/doi:10.1193/1.1585791.

[23] (BSSC) BSSC (2015): NEHRP Recommended seismic provisions for new buildings and other structures. vol. II.

[24] Seed HB, Idriss IM, Tokimatsu K (1986): Moduli and damping factors for dynamic analyses of cohesionless soils. Journal of Geotechnical Engineering, ASCE, 112 (11), 1016–1032.

[25] Kumar A, Mondal JK (2017): Newly Developed MATLAB Based Code for Equivalent Linear Site Response Analysis. Geotechnical and Geological Engineering, 35 (5), 2303–2325. https://doi.org/10.1007/s10706-017-



 

0246-4.

[26] Motazedian D, Atkinson GM (2005): Stochastic finite-fault modeling based on a dynamic corner frequency. Bulletin of Seismological Society of America, 95 (3), 995–1010.

[27] Atkinson GM, Silva W (1997): An empirical study of earthquake source spectra for California earthquakes. Bulletin of Seismological Society of Americal, 87 (1), 97–113.

[28] Chopra S, Kumar V, Suthar A, Kumar P (2012): Modeling of strong ground motions for 1991 Uttarkashi, 1999 Chamoli earthquakes, and a hypothetical great earthquake in Garhwal–Kumaun Himalaya. Natural Hazards, 64 (2), 1141–1159.

[29] Harbindu A, Gupta S, Sharma ML (2014): Earthquake ground motion predictive equations for Garhwal Himalaya, India. Soil Dynamics and Earthquake Engineering, 66, 135–148.

[30] Anbazhagan P, Kumar A, Sitharam TG (2013): Ground motion prediction equation considering combined dataset of recorded and simulated ground motions. Soil Dynamics and Earthquake Engineering, 53, 92–108.

[31] Harinarayan NH, Kumar A (2019): Estimation of source and site characteristics in the North-West Himalaya and its adjoining area using generalized inversion method. Annals of Geophysics, 62.

[32] Nath SK, Shukla K, Vyas M (2008): Seismic hazard scenario and attenuation model of the Garhwal Himalaya using near-field synthesis from weak motion seismometry. Journal of Earth System Science, 117 (S2), 649–670.

[33] Mukhopadhyay S, Kayal JR (2003): Seismic tomography structure of the 1999 Chamoli earthquake source area in the Garhwal Himalaya. Bulletin of Seismological Society of America, 93 (4),1854–1861.

[34] Banerjee S, Kumar A (2017): Determination of Seismic Wave Attenuation for the Garhwal Himalayas, India. Geosciences Research, 2(2), https://doi.org/10.22606/gr.2017.22005.

[35] Singh SK, Ordaz M, Dattatrayam RS, Gupta HK (1999): A spectral analysis of the 21 May 1997, Jabalpur, India, earthquake (Mw= 5.8) and estimation of ground motion from future earthquakes in the Indian shield region. Bulletin of Seismological Society of America, 89 (6), 1620-1630.

[36] Atkinson GM, Boore DM (2006): Earthquake ground-motion prediction equations for eastern North America. Bulletin of Seismological Society of America, 96, 2181–2205.



 